ELSEVIER

Biochimica et Biophysica Acta 1550 (2001) 129–143

BIOCHIMICA ET BIOPHYSICA ACTA
BBA

www.bba-direct.com

Formation of quasi-regular compact structure of poly(methacrylic acid) upon an interaction with α-chymotrypsin

Elena V. Kudryashova [a,*], Alexander K. Gladilin [a], Vladimir A. Izumrudov [a], Arie van Hoek [b], Antonie J.W.G. Visser [b], Andrey V. Levashov [a]

[a] *Chemistry Department, Moscow State University, 119899 Moscow, Russia*
[b] *MicroSpectroscopy Center, Department of Biomolecular Sciences, Wageningen University, Wageningen, Netherlands*

Received 22 February 2001; received in revised form 4 August 2001; accepted 3 September 2001

Abstract

Structure and dynamic properties of free poly(methacrylic acid) (PMA) and PMA complexed with α-chymotrypsin (CT) were studied using the time resolved fluorescence anisotropy technique. We have found that the interaction of PMA with CT induces the formation of a quasi-regular structure of PMA. At a CT/PMA weight ratio of 4:1 the interaction with CT leads to formation of approximately four equal segments of polyelectrolyte, each binding one CT molecule and characterized by an independent rotational mobility. Increase of the CT/PMA weight ratio above 8:1 gives rise to the overall rotation of the whole enzyme–polyelectrolyte complex. In water–ethanol mixtures the mobility of PMA segments containing CT decreases and the structure of the complex becomes even more rigid due to enhancement of the electrostatic interaction between CT and PMA. Formation of the compact and quasi-regular structure of the complex is perhaps the main reason behind the enhancement of enzyme stability and suppression of enzyme aggregation in water–organic cosolvent mixtures.

Keywords: α-Chymotrypsin; Pyrene-poly(methacrylic acid); Enzyme–polyelectrolyte complex; Time resolved fluorescence anisotropy

1. Introduction

Biocatalysis in extreme conditions such as high temperature, high hydrostatic pressure or organic solvent systems provides for multiple advantages in numerous practical areas including synthetic chemistry [1–7]. However, under such conditions, enzymes often lose their catalytic activity because of denaturation and/or aggregation and thus enzyme stabilization is often needed. It has been shown for enzymes of different classes [8–11] that non-covalent complex formation with polyelectrolytes is an effective method for enzyme stabilization in homogeneous water–organic cosolvent mixtures.

The influence of non-covalent complex formation with polyelectrolytes (PE) on the catalytic activity and the structure of α-chymotrypsin (CT) in water–organic cosolvent mixtures have been the subject of intensive studies during the last several years. It was

Abbreviations: PE, polyelectrolytes; CT, α-chymotrypsin; PMA, poly(methacrylic acid); TRFA, time resolved fluorescence anisotropy; A-CT, anthranil-CT; MOPS, 3-[*N*-morpholino]propanesulfonic acid

* Corresponding author. Chemical Enzymology dept., Faculty of Chemistry, M.V. Lomonosov Moscow State University, Vorobievy gory, Moscow 119899, Russia. Tel. 7/095/9393434 Fax: 7/095/9393429.

E-mail address: helena_koudriachova@hotmail.com (E.V. Kudryashova).

0167-4838/01/$ – see front matter
PII: S0167-4838(01)00274-6

demonstrated that free CT completely loses its catalytic activity at cosolvent concentrations of 30–50% v/v. In a water–ethanol system this inactivation is essentially due to protein aggregation and precipitation [8,9,12–19]. Formation of a complex with PE produces two major effects as compared to free enzyme [8,9]. (i) At cosolvent concentrations of 10–30% v/v CT–PE shows a pronounced activation (2–3-fold). (ii) The range of cosolvent concentrations where the enzyme retains its catalytic activity is much broader. The magnitude of both effects is independent of PE charge density and charge sign. It has been shown that behind this stabilization and activation effects are the maintenance of CT native conformation and suppression of enzyme aggregation and autolysis [8,9].

The structure of poly(methacrylic acid) (PMA) in aqueous solution has been extensively studied [20–23]. It is well accepted that in acidic medium PMA is characterized by a hypercoiled compact structure stabilized by hydrophobic interactions of α-methyl groups and formation of intramolecular H-bonds. In neutral media the dominating form of PMA is extended random coil. Nevertheless, upon these pH conditions several compact hydrophobic fragments of the specific structure are still present. At pH values above 8 the compact hydrophobic fragments in PMA are completely destroyed because of electrostatic repulsion of charged carboxylic groups. Good knowledge of PMA's spatial structure under various conditions makes a basis for studying the changes in the structural organization of PE induced by enzyme–PE complex formation.

Time resolved fluorescence anisotropy (TRFA) was chosen as the main method in these studies since it provides for detailed information on the spatial structure of the complex and allows following the internal and overall dynamics of the enzyme–polyelectrolyte complex. Independent sets of experiments were carried out to reveal the influence of CT on the PMA structure, as well as that of PMA on the CT structure upon complex formation. First, to study the structure and dynamic properties of PMA, PE was covalently modified with pyrene (pyrene-PMA). Pyrene is characterized by a long fluorescence lifetime and allows following relatively slow rotation, which can be expected for supramolecular structures such as enzyme–polyelectrolyte complex. Second, to study the influence of PMA on the structure and dynamic properties of CT, a fluorescent anthranil (A) group was introduced into the enzyme active site (formation of acyl enzyme). A-CT has no catalytic activity and is stable for months at neutral pH. The wavelengths of absorption and emission maximum of A-CT fluorescence (342 and 422 nm) are well removed from those of aromatic residues of the protein [24,25]. Due to this anthranilic label is very appropriate for this study.

The aim of the present study was to characterize the structure of enzyme–polyelectrolyte complexes and to reveal its relationship with the catalytic activity of the enzyme in water–organic cosolvent systems.

2. Materials and methods

2.1. Chemicals

Bovine pancreatic α-chymotrypsin and *p*-nitroanilide anthranilate were from Sigma. Ethanol Uvasol was from Merck. Water was purified on a Millipore system. All other reagents were of analytical grade.

2.2. Preparation of the enzyme–PE complexes

The complexes of CT with PMA (molecular mass of 300 kDa) were prepared by mixing solutions of the enzyme and the polyelectrolyte both dissolved in 5 mM aqueous buffer of 3-[*N*-morpholino]propanesulfonic acid (MOPS), pH 7.45 [8,9]. The CT/PMA weight ratio was varied from 1:1 to 32:1 (molar ratio from 12:1 to 384:1).

2.3. Synthesis of pyrene-PMA

Synthesis of pyrene-PMA was performed as previously described in [26] (the modification degree was 5).

2.4. Covalent labeling of α-chymotrypsin

α-Chymotrypsin was modified with *p*-nitroanilide anthronilate according to [27]. The active site concentration of the modified enzyme was less than 5% of that of native CT. The assay was carried out with *N-trans*-cinnamoylimidazole [9,28].

2.5. Fluorescence measurements

Steady-state fluorescence spectra were recorded on a SLM-Aminco SPF-500C fluorimeter. For all experiments the excitation wavelength was 340 nm. Steady-state fluorescence anisotropy was measured on a T-format steady-state fluorescence polarimeter with dual-channel photon counting. Excitation wavelength was 340 nm. The 360 nm cutoff filter was used for emission detection.

Time resolved fluorescence and fluorescence anisotropy decays were measured using the time-correlated single-photon-counting technique, which is summarized for application in [29–31]. The excitation source consisted of the frequency-doubled output of a cavity-dumped dye laser, which was synchronously pumped by a mode-locked Antares 76-YLF laser (Coherent, Palo Alto, CA, USA). The excitation wavelength was 343 nm. As the laser dye [4-dicyanomethylene-2-methyl-6-(*p*-dimethylaminostyryl)-4*H*-pyran] was used. The frequency of excitation pulses was 951.2 kHz for experiments with A-CT and 475.6 kHz for experiments with pyrene-PMA. For A-CT fluorescence a combination of a KV380 cutoff filter (Schott) with a 402 nm interference filter (Baird Atomic) was used. In the case of pyrene-PMA a KV380 cutoff filter and a 392.1 nm interference filter (both Schott) were used. The reference compound was a solution of POPOP (Eastman Kodak) in fluorescence grade ethanol characterized by a fluorescence lifetime of 1.35 ns [24]. One complete experiment consisted of measuring the polarized (parallel and perpendicular component) fluorescence decays of the reference compound (three cycles of 20 s), the sample (10 cycles of 20 s), the background (two cycles of 20 s), and again the reference compound. We have acquired the fluorescence data using 16.32 and 30.42 or 46.05 ps/channel for the experiments with A-CT and pyrene-PMA, respectively. Decay curves consisted of 4000 channels each in the case of A-CT and 2000 channels in the case of pyrene-PMA. Overall concentrations of A-CT and pyrene-PMA were 1.2 and 0.04 mM, respectively. Full details of the data analysis have been given previously [24,30,31]. All experiments in this work were carried out at 20°C.

Examples of experimental and fitted fluorescence and anisotropy decays are given for the case of CT–pyrene-PMA complex at a CT/PMA weight ratio of 10:1 in aqueous solution (Fig. 1A,B).

2.6. Circular dichroism

Circular dichroism experiments in the far-ultraviolet region (195–260 nm) were carried out with a Jasco J-715 spectrometer at 25°C with quartz cells of path length 1 mm. The protein concentration was 4 μM.

3. Results

3.1. Steady-state fluorescence of pyrene-PMA and CT–pyrene-PMA

The fluorescence emission spectrum of pyrene-PMA in aqueous solution is characterized by two sharp peaks at 379 and 398 nm and by a shoulder at 418 nm (Fig. 2). Such a spectrum is usually referred to the pyrene monomer [21,32]. No excimer emission is observed, indicating that the pyrene moieties are not in molecular contact. Introduction of ethanol into the system results in higher intensity of all peaks in the spectrum, maximal values being observed at 50% v/v of ethanol (Fig. 3). Besides, at ethanol concentrations above 50% v/v definite destructurization of the spectrum is observed (Fig. 2). All these results imply dramatic changes in the polarity of the environment of the pyrene groups [21,33] due to structural reorganization in PMA.

The complex formation with CT leads to a decrease in fluorescence intensity of pyrene-PMA in aqueous solution and in the whole range of the solvent composition (Fig. 3). This can be due to a quenching of the pyrene dyes by bound CT molecules and/or compactization of PMA induced by the complex formation (see below, Tables 1 and 3). The quenching efficiency rises with the increase of CT/PMA weight ratio, which implies further compactization of PMA.

3.2. Steady-state fluorescence anisotropy of pyrene-PMA and CT–pyrene-PMA

The steady-state fluorescence anisotropy of free pyrene-PMA in aqueous solution and water–ethanol mixtures with low ethanol content is about 0.005

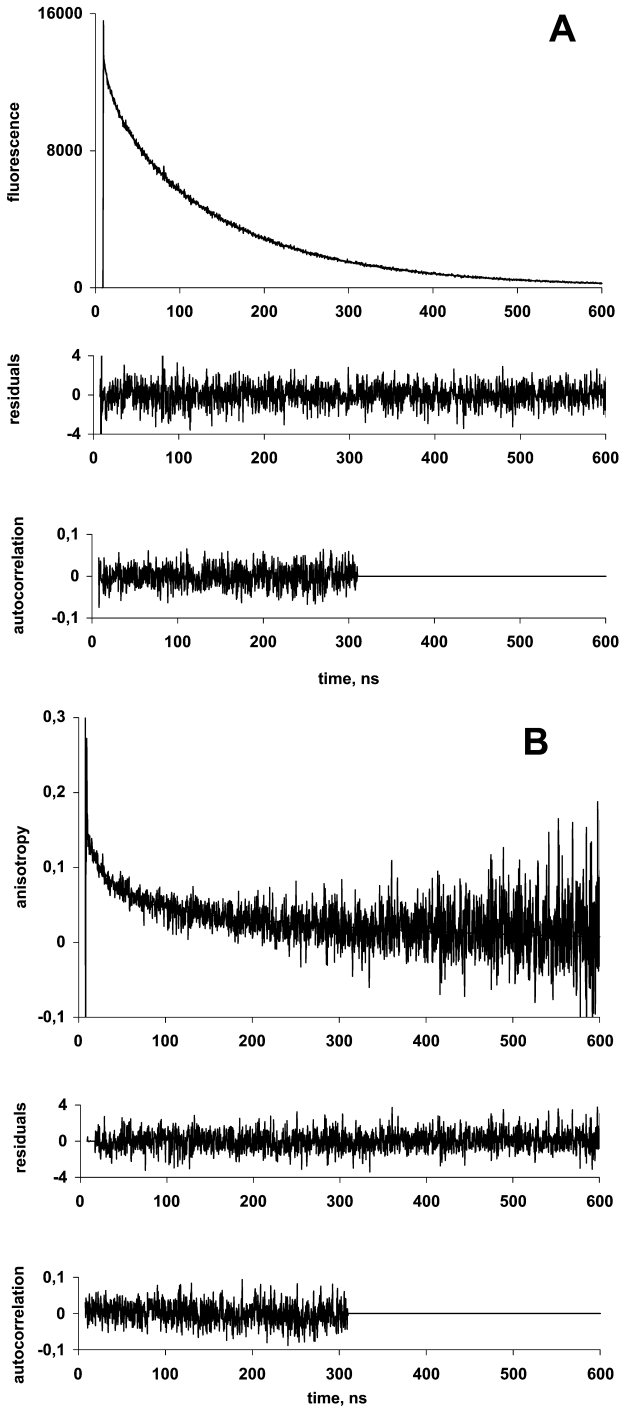

Fig. 1. Experimental total fluorescence decay (A) and fluorescence anisotropy decay of CT–pyrene-PMA at a CT/PMA weight ratio of 10:1 in aqueous solution. Excitation wavelength 343 nm, emission wavelength 393 nm. Experimental conditions: 5 mM MOPS buffer, pH 7.5; temperature 20°C. Estimated fluorescence and anisotropy decay parameters and their confidence intervals at the 67% level:

α_1	τ_1	α_2	τ_2	α_3	τ_3
0.10	12.5 (12.1–12.7)	0.20	80.5 (76.2–83.5)	0.37	175 (172–179)
β_1	ϕ_1	β_2	ϕ_2	β_3	ϕ_3
0.27	0.31 (0.27–0.35)	0.08	28.7 (26.4–30.4)	0.06	278 (269–290)

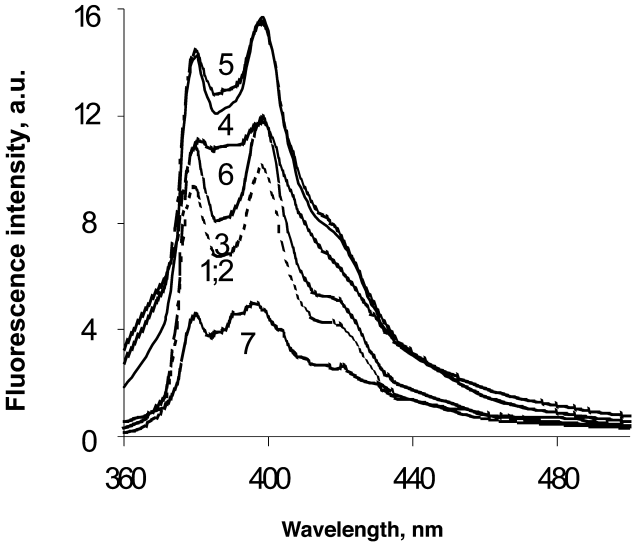

Fig. 2. Fluorescence spectra of pyrene-PMA in water–ethanol mixtures. Excitation wavelength 340 nm. Ethanol concentrations (% v/v): (1) 0; (2) 10; (3) 30; (4) 40; (5) 50; (6) 60; (7) 80. Experimental conditions: 5 mM MOPS buffer, pH 7.5; temperature 20°C; [pyrene-PMA] 0.04 μM.

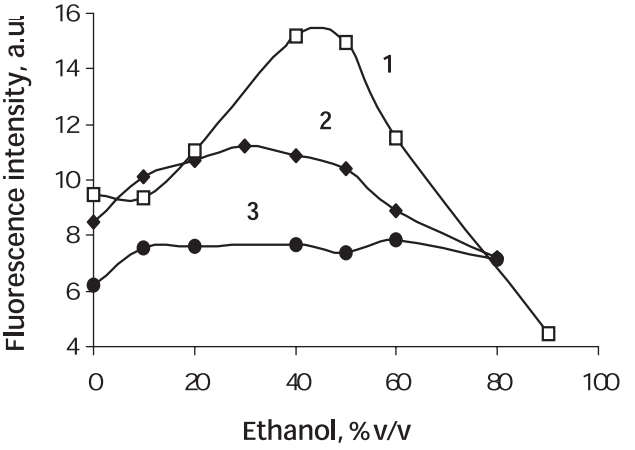

Fig. 3. Fluorescence intensity of free pyrene-PMA (1), CT–pyrene-PMA (2, 3) as a function of ethanol concentration. CT/PMA weight ratios 4:1 (2) and 10:1 (3). Excitation wavelength 340 nm. Other experimental conditions as in Fig. 2.

(Fig. 4), which indicates a high mobility of the pyrene groups in PMA. At ethanol concentrations above 40% v/v the fluorescence anisotropy of pyrene-PMA gradually increases reflecting increased rigidity of the PMA structure. Most likely, this growth of the rigidity is conditioned by neutralization of the negative charges of PMA by low molecular weight counterions substantially enhanced by the lowering of the solvent polarity.

In aqueous solution the complex formation with CT and the increase of the CT/PMA weight ratio lead to the successive increase in fluorescence anisotropy of pyrene-PMA (Fig. 4). The 'loading' of the polyanion with CT results in the involvement of more and more free charged segments of PMA in complex with CT. Accordingly, the average mobility of the pyrene dyes goes down and the fluorescence anisotropy goes up. The maximal value of anisotropy (0.15) is observed for the complex with CT/PMA weight ratio of 32:1 (molar ratio 384:1, charge ratio 2:1). A further increase of the CT/PMA ratio was followed by precipitation, indicating the formation of a stoichiometric complex in which virtually all carbolylate groups of PMA form salt bonds with the accessible amine groups of CT. The estimated dissociation constant (K_{dis}) for the soluble complex is approx. 20–50 base μM (Fig. 4 insert) (taking into account that the number of amino groups in CT is 16).

In water–ethanol mixtures CT–pyrene-PMA obey the same trend in increase in anisotropy with increase in ethanol content as was observed for pyrene-PMA

Table 1
Fluorescence lifetimes (τ) and their relative contributions (α) for pyrene-PMA as a function of ethanol concentration

Ethanol (% v/v)	α_1	τ_1 (ns)	α_2	τ_2 (ns)	α_3	τ_3 (ns)
0	0	0	0.09	53	0.67	140
18	0	0	0.08	58	0.68	166
40	0.08	10.2	0.08	85	0.57	180
47	0.04	14.0	0.10	81	0.63	173
50	0.07	11.4	0.09	76	0.59	167
60	0.07	17.5	0.32	107	0.38	177
80	0.15	20.3	0.40	90	0.22	191

Excitation wavelength 340 nm, emission wavelength 393 nm.

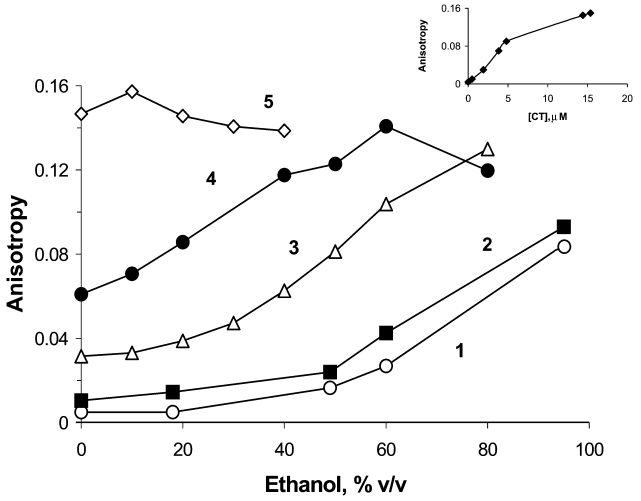

Fig. 4. Steady-state fluorescence anisotropy (excitation wavelength 340 nm) of pyrene-PMA (1) and CT–pyrene-PMA (2–5) as a function of ethanol concentration. CT/PMA weight ratios: (2) 1:1; (3) 4:1; (4) 8:1; (5) 32:1. (Insert) Steady-state fluorescence anisotropy of CT–pyrene-PMA in aqueous solution as a function of CT concentration. Experimental conditions as in Fig. 2.

(Fig. 4). For the complexes the growth of the anisotropy is more pronounced. At a CT/PMA weight ratio of 32:1 (charge ratio 2:1) the anisotropy is practically constant in the whole range of the solvent composition, which implies that at this ratio the free charged PMA segments are practically exhausted and the saturation of PMA with CT is achieved. All these results can be readily explained by the same influence of environment polarity on electrostatic interaction. It is apparent that the higher the CT/PMA ratio, i.e. the greater the number of CT molecules that formed salt bonds with the PE matrix, the smaller are the number and length of the non-occupied PMA segments. Accordingly, the more sensitive should be the mobility of the complex domains to the strengthening of its electrostatic interaction with counterions. Moreover, it is not inconceivable that for the same reason, i.e. lowering the medium polarity, the electrostatic interactions between the enzyme and the polyanion are enhanced, promoting the increase in complex rigidity.

3.3. Steady-state fluorescence of A-CT and A-CT–PMA

The fluorescence emission spectra of A-CT and A-CT–PMA were examined as a function of ethanol concentration to monitor conformational changes associated with polarity changes in the CT active site. The fluorescence spectrum of A-CT in aqueous solution has a maximum at 422 nm, which is in good agreement with previously obtained data [24,25,27]. With increasing ethanol concentration up to 40% v/v, the fluorescence intensity of A-CT and the value of λ_{max} increase (Fig. 5). For free anthranil compounds the value of λ_{max} in organic solvents (such as methanol, acetonitrile, etc.) decreases compared to aqueous solutions [27]. All this implies that ethanol induces some perturbances in the enzyme active site conformation towards the more open one. In the range of ethanol concentrations from 40 to 90% v/v the wavelength of the maximal emission (λ_{max}) is practically constant (curve 1 in Fig. 5B). The latter can be explained by enzyme aggregation, which has been observed at the given conditions by other methods [9,17–19].

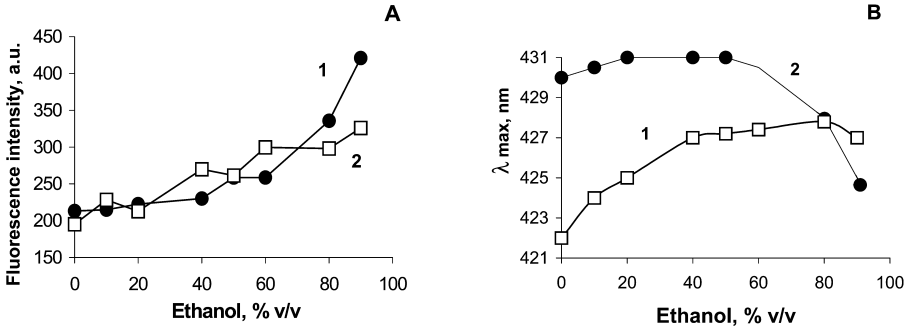

Fig. 5. Fluorescence intensity (A) and wavelength of maximal emission (B) of free A-CT (1) and A-CT–PMA (2) as a function of ethanol concentration. Excitation wavelength 340 nm. Experimental conditions: 5 mM MOPS buffer, pH 7.5; temperature 20°C; [A-CT] = 1.2 μM; [PMA] = 0.04 μM.

The fluorescence emission spectrum of A-CT–PMA in aqueous solution is characterized by a maximum at 430 nm (curve 2 in Fig. 5B). The pronounced red shift of λ_{max} upon complex formation indicates a drastic increase in medium polarity in the vicinity of the emitting anthranilic group [27]. The fluorescence intensity and λ_{max} of A-CT–PMA remain practically constant with an increase in ethanol concentration up to 60% v/v. This could be expected since, as mentioned above, the addition of ethanol could only enhance the electrostatic interaction of CT with PMA. In other words, the complex formation with PMA reliably protects the active site of CT from the contact with the solvent molecules. At ethanol concentrations above 60% v/v λ_{max} starts to decrease due to aggregation (data shown below, Tables 4 and 6).

3.4. Time-resolved fluorescence of pyrene-PMA in aqueous solution and water–ethanol mixtures

In aqueous solution and at low ethanol concentrations pyrene-PMA is characterized by two populations of pyrene groups (fluorescence lifetimes τ_2 and τ_3 of 50 and 140 ns, Table 1). The major contribution to the total fluorescence decay is provided by the longer fluorescence lifetime (τ_3). This value is attributed to pyrene monomers in polar media [33–35] and can be assigned to pyrene groups of PMA exposed to the solution. The fluorescence lifetime (τ_2) could correspond to inner pyrene groups in PMA included in the interaction with hydrophobic fragments existing in free PMA at neutral pH values [20–23]. The values of both these fluorescence lifetimes have a noticeable tendency to go up with increasing ethanol concentration due to lowering of the medium polarity. The relative contribution of lifetime (τ_2) rises significantly at ethanol concentrations above 50% v/v at the expense of τ_3. The shortest fluorescence lifetime (τ_1) makes same contribution only at an ethanol concentration of 80% v/v. The appearance of τ_1 is likely to reflect the formation of a collapsed structure of PMA at high ethanol concentrations [20–23], leading to quenching of a small amount of pyrene groups. All these findings are evidence in favor of the above assumption that the lowering of medium polarity leads to neutralization of PMA free segments and promotes the intramolecular hydrophobic interactions.

3.5. Rotational dynamics of PMA in aqueous solution and water–ethanol mixtures

Pyrene-PMA shows two types of rotational motion: rapid rotation of pyrene groups around the point of attachment (rotational correlation time ϕ_1 in Table 2) and motion of a hydrophobic fragment of PMA (rotational correlation time ϕ_2 in Table 2). Both correlation times (ϕ_1 and ϕ_2) increase with an increase in ethanol content and peak at an ethanol concentration of 47%, which corresponds to minimal rotational mobility of the hydrophobic fragments in PMA and pyrene groups around the point of attachment. All this implies the enhancement of intramolecular hydrophobic interactions. On further increasing the ethanol concentration, the

Table 2
Anisotropy decay parameters: rotational correlation times (ϕ) and their relative contributions (β) for pyrene-PMA as a function of ethanol concentration

Ethanol (% v/v)	β_1	ϕ_1^a	β_2	ϕ_2^b	β_3	ϕ_3^c
0	0.20	0.3	0.08	5.1	–	–
18	0.17	0.5	0.10	8.0	–	–
40	0.13	1.1	0.10	12.2	–	–
47	0.09	2.2	0.09	16.4	–	–
50	0.16	0.7	0.11	12.3	–	–
60	–	–	0.10	9.6	0.04	210
80	–	–	0.04	7.4	0.14	>1000

Excitation wavelength 343 nm, emission wavelength 393 nm.
[a]Rotation of pyrene group around the point of attachment.
[b]Motion of hydrophobic fragments of PMA.
[c]Motion of PMA aggregates.

relative contribution of both types of motion to anisotropy decay decreases. This region of the solvent composition corresponds to aggregation of PMA molecules. The aggregation is evident from the appearance of the longest correlation time (ϕ_3) (unresolved on the nanosecond time scale), corresponding to very slow rotation of PMA intermolecular associates.

3.6. Time-resolved fluorescence of CT–pyrene-PMA in aqueous solution and water–ethanol mixtures

Complex formation with enzyme causes drastic conformational changes of PMA. Some of the pyrene groups of PMA free charged segments initially exposed to the solution (τ_3 in Table 1) become involved in inner hydrophobic regions of the complex (τ_2 in Table 3). Accordingly, as compared to free pyrene-PMA, the relative contribution of τ_2 to the complex increases at the expense of τ_3 (Table 3).

The pyrene groups of PMA hydrophobic fragments (τ_2 in Table 1) are transferred to inner hydrophobic regions of the complex as well (τ_2 in Table 3). Accordingly, the value of τ_2 in the CT–PMA complex is greater as compared to that of free PMA (compare τ_2 in Table 1 and τ_2 in Table 3). Moreover, the hydrophobic fragments of PMA and CT–PMA hydrophobic regions could effectively interact with one another. All this could be expected, as upon complex formation the hydrophobic inner regions consisting of electrostatically bound components are usually formed (for review see [36]).

Finally, the pyrenes with the shortest lifetime (τ_1) came up with complex formation. These are probably the pyrenes interacting very tightly with their environment, which results in quenching of the fluorescence. Thus, one can judge that the structure of the PMA–CT complex is quite compact.

The values τ_1 and τ_2 and their relative contributions are practically independent on ethanol concentration (Table 3A). The value of τ_3 increases with the increase in ethanol concentration as was observed in the case of free pyrene-PMA. All these results indicate that the structure of the complex is quite stable in water–ethanol mixtures.

In the system with higher CT content (CT/PMA weight ratio 10:1, molar ratio 120:1) both τ_1 and τ_2 are characterized by smaller values (Table 3B). This can be explained by a more compact CT–pyrene-PMA structure when more CT molecules are complexed to PMA, leading to a slight quenching of the pyrene fluorescence.

3.7. Rotational dynamics of CT–pyrene-PMA in aqueous solution and water–ethanol mixtures

The rotational dynamics of PMA change markedly upon complex formation with the enzyme and reveal a pronounced dependence on the CT/PMA weight ratio (Table 4A,B). In aqueous solution the forma-

Table 3
Fluorescence lifetimes (τ) and their relative contributions (α) for CT–pyrene-PMA at CT/PMA weight ratios of 4:1 (A) and 10:1 (B)

Ethanol (% v/v)	α_1	τ_1	α_2	τ_2	α_3	τ_3
(A)						
0	0.07	21.0	0.36	112	0.32	176
18	0.06	23.0	0.15	108	0.53	181
47	0.07	17.1	0.23	116	0.46	203
60	0.09	19.0	0.30	113	0.39	212
80	0.10	30.5	0.01	104	0.30	220
(B)						
0	0.10	12.45	0.20	81	0.37	175
10	0.10	10.72	0.20	96	0.36	193
20	0.10	7.62	0.13	66	0.49	185
30	0.10	8.74	0.13	81	0.50	199
40	0.23	10.51	0.06	87	0.20	205
50	0.10	14.47	0.16	87	0.50	205
60	0.12	10.66	0.18	79	0.46	207
70	0.17	12.45	0.04	91	0.05	213

Excitation wavelength 343 nm, emission wavelength 393 nm.

Table 4
Rotational correlation times (ϕ) and their relative contributions (β) for CT–pyrene-PMA at CT/PMA weight ratios of 4:1 (A) and 10:1 (B) as a function of ethanol concentration

(A)						
Ethanol (% v/v)	β_1	ϕ_1^a	β_2	ϕ_2^b	β_3	ϕ_3^c
0	0.10	3.3	0.06	59	–	–
18	0.10	5.6	0.05	92	–	–
47	0.08	5.4	0.05	62	0.06	>1000
60	–	–	0.04	33	0.11	>1000
80	0.01	5.5	0.02	11	0.15	>1000

(B)								
Ethanol (% v/v)	β_1	ϕ_1^d	β_2	ϕ_2^b	β_3	ϕ_3^e	β_4	ϕ_4^c
0	0.27	0.3	0.08	28.7	0.06	278	–	–
10	0.30	0.4	0.08	40.7	0.08	403	–	–
20	0.24	0.3	0.05	39.8	0.08	577	–	–
30	–	–	–	–	0.06	167	0.05	>1000
40	–	–	–	–	0.03	164	0.09	>1000
50	0.17	0.3	0.03	44.5	0.05	146	0.13	>1000
60	0.15	0.2	0.02	10.7	–	–	0.15	>1000
70	–	–	–	–	–	–	0.15	>1000

Excitation wavelength 343 nm, emission wavelength 393 nm.
[a]Motion of hydrophobic fragments of PMA.
[b]Rotation of PMA segments containing CT.
[c]Motion of the CT–PMA aggregates.
[d]Rotation of pyrene group around the point of attachment.
[e]Motion of whole CT–PMA.

tion of an enzyme–polyelectrolyte complex with a CT/PMA weight ratio of 4:1 (molar ratio 48:1) gives rise to a rotational correlation time (ϕ_2) of 60 ns (Table 4A). This value allows one to attribute ϕ_2 to the rotational motion of several (approximately four) PMA segments of equal size, containing one molecule of enzyme. So, the stoichiometric ratio of CT/PMA at current conditions could be estimated as 4:1. In water–ethanol mixtures the distinct maximum of correlation time ϕ_2 is observed at an ethanol concentration of 18% v/v (Table 4A), which corresponds to the lowest mobility of PMA segments containing CT. The longest rotational correlation time (ϕ_3) registered at ethanol concentrations above 47% v/v can reflect the formation of aggregates of the complex.

An increase in the CT content in the system up to a CT/PMA weight ratio of 10:1 leads to a shorter correlation time (ϕ_2) (Table 4B). This can be due to an increased number of PMA segments containing CT. The longest correlation time (ϕ_3) (of 280 ns in aqueous solution) can be attributed to the overall rotation of the CT–PMA complex. Based on this

Table 5
Fluorescence lifetimes (τ) and their relative contribution (α) for A-CT (A) and A-CT–PMA (B) as a function of ethanol concentration

Ethanol (% v/v)	α_1	τ_1	α_2	τ_2
(A)				
0	0.42	5.5	0.48	10.3
10	0.35	5.5	0.55	10.0
20	0.25	5.3	0.65	9.8
40	0.26	5.9	0.64	9.9
50	0.18	5.9	0.72	9.8
60	0.24	6.4	0.66	10.0
80	0.21	6.7	0.69	10.0
(B)				
0	0.48	5.5	0.44	9.6
10	0.31	5.2	0.62	9.3
20	0.20	5.2	0.71	9.5
40	0.18	5.5	0.74	9.8
50	0.18	5.4	0.73	10.0
60	0.19	5.7	0.71	10.1
80	0.29	7.2	0.59	10.4

Excitation wavelength 343 nm, emission wavelength 393 nm. Experimental conditions: 5 mM MOPS buffer, pH 7.5; temperature 20°C; [A-CT] = 1.2 μM; [PMA] = 0.04 μM.

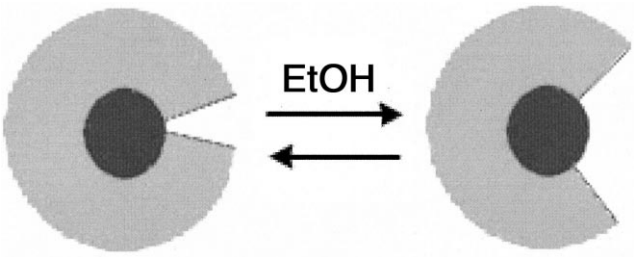

Fig. 6. Influence of ethanol on CT active site microenvironment. A-CT is characterized by two distinct substates of the protein with different environment of the anthranilic group. Ethanol induces a shift towards the substate with higher accessibility of the active site.

value and on the assumption of a compact spherical structure of the complex we estimated the molecular mass of the complex as it is described elsewhere [25,34,37]. The resulting molecular mass of 600 kDa corresponds to a CT/PMA stoichiometric ratio of 10:1. These findings suggest noticeable transformation of the system caused by the 'loading' of PMA matrix with CT, namely, the overall rotation of the complex emerges. This also could point to the compactization of the complex structure and enhancement of the interaction between PMA segments containing CT.

At an ethanol concentration of 20% v/v minimal mobility of the overall structure of the CT–PMA complex is observed. This can be judged from a distinct maximum of the long correlation time (ϕ_3) at this ethanol concentration (Table 4B). The longest unresolved rotational correlation time (ϕ_4) can be attributed to the motion of aggregates of the complex.

3.8. *Time-resolved fluorescence of anthranil-CT and anthranil-CT–PMA in aqueous solution and water–ethanol mixtures*

A-CT is characterized by two fluorescence lifetimes

Table 6
Rotational correlation times (ϕ) and their relative contributions (β) of A-CT (A) and A-CT–PMA (B) as a function of ethanol concentration

(A)						
Ethanol (% v/v)	β_1	ϕ_1^a	β_2	ϕ_2^b	β_3	ϕ_3^c
0	0.32	12.5	–	–	–	–
10	0.18	13.1	0.14	36.3	–	–
20	0.11	12.6	0.21	49.2	–	–
40	0.03	11.0	0.40	53.4	–	–
50	–	–	0.18	51.6	0.10	>1000
60	0.06	8.1	–	–	0.24	>1000
80	0.03	4.8	–	–	0.24	>1000
(B)						
Ethanol (% v/v)	β_1	ϕ_1^d	β_2	ϕ_2^e	β_3	ϕ_3^f
0	0.13	16.9	0.15	96	–	–
10	0.13	16.4	0.20	145	–	–
20	0.14	22.0	0.14	600	–	–
40	0.03	11.0	0.24	147	–	–
50	–	–	0.32	186	–	–
60	0.02	7.8	–	–	0.30	>1000
80	0.03	4.5	–	–	0.26	>1000

Experimental conditions as in Table 5.
[a]Rotation of A-CT.
[b]Rotation of trimer and tetramer of A-CT.
[c]Motion of large A-CT aggregates.
[d]Rotation of A-CT interacting with hydrophobic fragment of PMA.
[e]Rotation of A-CT interacting with large segment of PMA.
[f]Motion of large A-CT-PMA aggregates.

of 5.5 and 10 ns (Table 5A), which reflects the existence of two substates of the CT active site differing in polarity and accessibility (Fig. 6). A similar result was obtained previously [24,25]. The values of both lifetimes (τ_1 and τ_2) are practically independent of ethanol concentration. Hence, the same two substates are present in water–ethanol mixtures. The relative contribution of the longer lifetime increases approx. 1.5-fold when the ethanol concentration in the system is increased. Thus, ethanol induces a shift towards the substate with higher accessibility of the active site (Fig. 6). A similar conclusion is also drawn from the dependence of the fluorescence λ_{max} of A-CT on the ethanol concentration (Fig. 5B).

Complex formation with PMA at a CT/PMA weight ratio of 1:1 (molar ratio 12:1) has only a marginal effect on the fluorescence lifetime distribution of A-CT and consequently on the equilibrium between the substates of the CT active site in aqueous solution and water–ethanol mixtures (Table 5B).

3.9. *Rotational dynamics of anthranil-CT and anthranil-CT–PMA in aqueous solution and water–ethanol mixtures*

In aqueous solution A-CT is characterized by only one type of rotation motion: rotation of the whole protein molecule (rotational correlation time $\phi_{prot.}$ of 12.4 ns, Table 6A). A similar value was reported earlier for A-CT [24,25]. Addition of ethanol gives rise to a longer correlation time (ϕ_2), which implies that ethanol induces the formation of CT aggregates. At an ethanol concentration of 10% v/v, the value of the long correlation time of 36 ns corresponds well to rotational motion of a dimer. At ethanol concentrations of 20–50% v/v, the long correlation time increases up to 49–53 ns, which corresponds to tetramer rotational motion. At ethanol concentrations higher than 50% v/v, the longest unresolved rotational correlation time appears, which reflects the formation of large protein aggregates.

In aqueous solution, complex formation of A-CT with PMA gives rise to correlation times ϕ_1 and ϕ_2 of 17 and 96 ns (Table 6B). One can assume that ϕ_1 of 17 ns reflects the rotation of A-CT surrounded by hydrophobic fragments of PMA (taking into consideration the values of correlation times attributed to PMA hydrophobic fragments (Table 2) and to A-CT (Table 6A)). The long correlation time (ϕ_2) can be assigned to the rotational motion of A-CT bound with large PMA segments (approximately half of the PMA molecule). Both correlation times (ϕ_1 and ϕ_2) are maximal at an ethanol concentration of 20% v/v, indicating the lowest mobility of both the small and large segments of PMA interacting with A-CT. The absence of a correlation time in the range of 36–50 ns indicates that complex formation suppresses protein aggregation in water–ethanol mixtures, which is in good agreement with previously reported results [9].

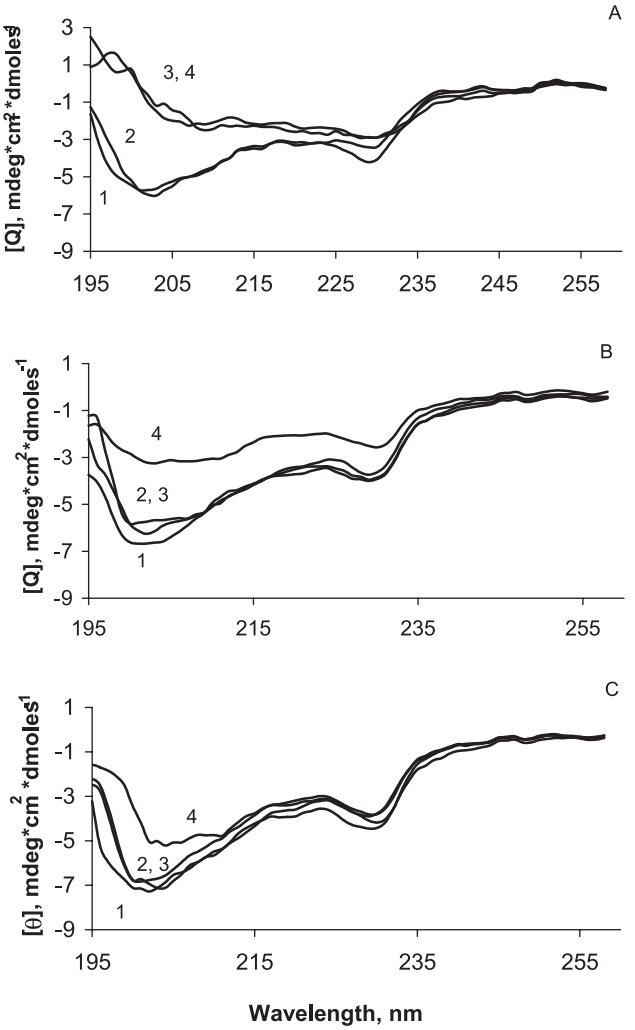

Fig. 7. CD spectra in the far-UV region for free CT (A) and CT–PMA (B,C) as a function of ethanol concentration. CT/PMA weight ratios: 1:2.5 (B) and 4:1 (C). Ethanol concentrations (% v/v): (A) 1, 0; 2, 20; 3, 30; 4, 50; (B,C) 1, 0; 2, 20; 3, 50; 4, 70. Experimental conditions: 5 mM MOPS buffer, pH 7.5; temperature 20°C; [CT] = 4 μM.

3.10. Circular dichroism (CD) spectroscopy in far-UV region

3.10.1. Aqueous solution

The CD spectrum of CT in aqueous solution shows a negative maximum at 230 nm, a shoulder at 222 nm, and a negative band at 203 nm (curve 1 in Fig. 7A). The spectrum is similar to that reported in [9,12]. Spectral analysis gives 10–12% of α-helix and 32–34% of β-sheets (Table 7).

In aqueous solution the complex CT–PMA at CT/PMA weight ratios of 1:2.5 and 4:1 is characterized by a native-like secondary structure (Fig. 7B,C). It should be stressed that PMA has a negligible CD spectrum in the far-UV region.

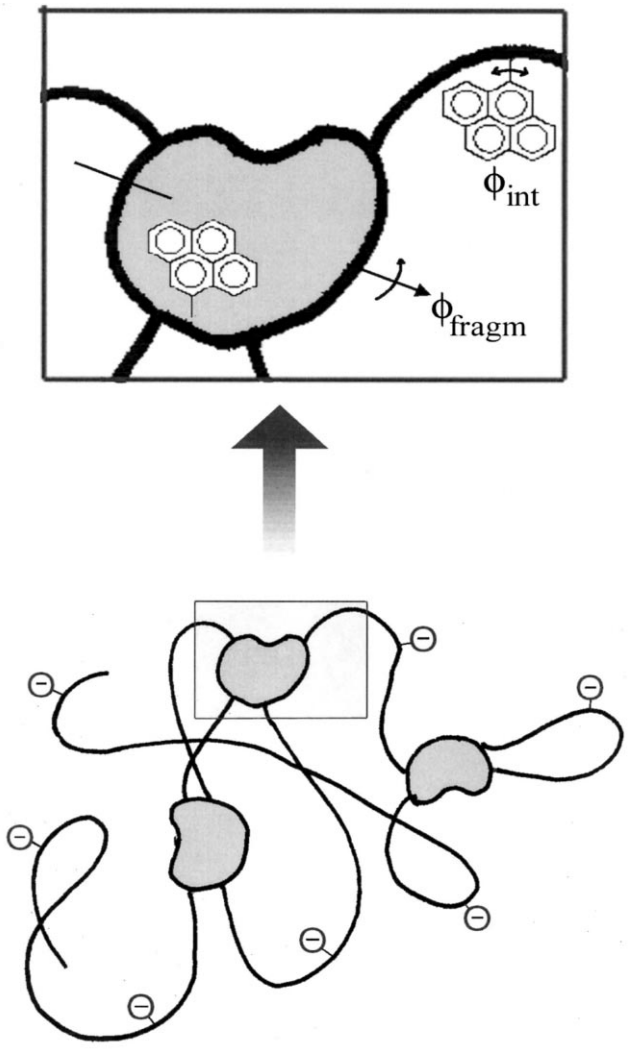

Fig. 8. Supposed structure of pyrene-PMA. The gray figures are the hydrophobic fragment.

3.10.2. Water–ethanol mixtures

Addition of small amounts of ethanol (up to 20% v/v) has only a marginal influence on the secondary structure of the protein for both free CT and CT–PMA (curves 2, Fig. 7A–C). At ethanol concentrations of 30% v/v and higher ethanol induces dramatic changes in the secondary structure of free CT: a significant decrease in ellipticity at 230 and 203 nm (curves 3 and 4 in Fig. 7A) reflecting lower contents of α-helix (Table 7) [38,39].

A similar decrease in the ellipticity of the CD spectrum of CT–PMA with a weight ratio of 1:2.5 at 230 nm and 203 nm is observed at an ethanol concentration as high as 70% v/v (curve 4 in Fig. 7B). Hence, complex formation with PMA results in broadening by 40% v/v the range of ethanol concentrations where CT retains a native-like secondary structure.

Increasing the CT/PMA weight ratio to 4:1 results in even further stabilization of the enzyme secondary structure. For instance, at an ethanol concentration of 70% v/v the decrease in ellipticity at 230 and 203 nm in the CD spectrum is not so dramatic (curve 4 in Fig. 7C). Such an effect of the complex composition on the stability of the CT secondary structure can be due to the formation of a more rigid structure of the complex at high CT/PMA ratio. We observed the same tendency when using TRFA.

4. Discussion

4.1. Influence of CT on PMA structure

In aqueous solution at pH 7.5 PMA exists as an extended random coil containing several compact fragments stabilized by hydrophobic interactions of α-methyl groups and intramolecular H-bonds [20–23]. According to the relative contribution of the corresponding lifetime (τ_2 in Table 1) to the total fluorescence decay of pyrene-PMA, about 10% of PMA units are involved in the formation of such compact hydrophobic fragments. Analysis of the time-resolved anisotropy decay of pyrene-PMA suggests that the molecular mass of these fragments is about 10 kDa. Hence, each PMA molecule at pH 7.5

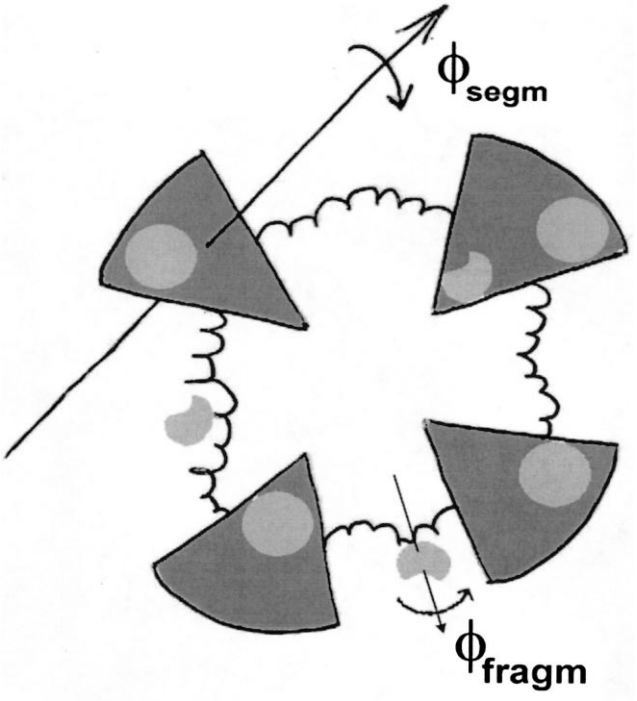

Fig. 9. Supposed structure of CT–PMA at a CT/PMA weight ratio of 4:1. Gray circle, CT; gray half-circle, hydrophobic fragment.

may contain about three hydrophobic fragments (Fig. 8).

We have found that in the complex CT–PMA at a CT/PMA weight ratio of 1:1 (molar ratio 12:1), CT interacts with one of the hydrophobic fragments of PMA. Besides, a large segment of PMA (about half of the molecule) is involved in electrostatic interaction with each enzyme molecule (ϕ_1 and ϕ_2 in Table 6B). The size of PMA segments interacting with CT increases on addition of ethanol to the system (ϕ_2 in Table 6B), which could be due to enhancement of electrostatic interactions.

Increasing the CT/PMA ratio up to 4:1 (molar ratio 48:1) induces the formation of a more compact structure, composed of approximately four PMA segments of equal size, each containing one CT molecule surrounded by a PMA chain (Fig. 9, Tables 3 and 4).

A further increase in the CT/PMA ratio up to 10:1 (molar ratio 120:1) results in the formation of approx. 10 segments of equal size per PMA molecule, each containing one CT molecule (ϕ_2 in Table 4B). The high rigidity of such segments and the low amount of free charges in PMA lead to the formation of the overall structure of the complex. This is supported by the appearance of the overall rotational correlation time of the complex (ϕ_3 in Table 4B). A similar tendency was observed for the complex with a CT/PMA weight ratio of 8:1.

At a CT/PMA weight ratio of 32:1 (molar ratio 400:1), saturation of PMA with CT is achieved, since the steady-state anisotropy no longer changes at increasing ethanol concentration (Fig. 4). At higher CT/PMA initial ratios or at ethanol concentrations above 50%, formation of a non-soluble complex takes place due to compensation of most charges on PMA.

The distribution of CT to the complex does not obey an 'all or nothing' principle. If the 'all or nothing' principle is true, at all CT/PMA initial ratios one would expect to observe dynamic properties of free PMA and of the complex with maximal CT/PMA ratio, usually referred to as the 'characteristic composition'. However, the dynamic properties attributed to free pyrene-PMA are not detected even at CT/PMA weight ratios as low as 4:1 (Table 4A) and a strong dependence of CT–PMA dynamics on the CT/PMA initial ratio is observed (Table 4A,B).

Table 7
Percentage of secondary structure elements, estimated from CD spectra using CDNN software (http://bioinformatik.biochemtech.uni-alle.de/cd_spec/cdnn)

Sample	EtOH (%)	α-Helix	β-Sheets	β-Turn	Random coil
CT theoretical data[a]	0	10	34	20	36
CT experimental data	0	10.7	32.6	22.3	34.4
	20	10.3	32.0	22.6	35.1
	30	7.5	38.8	19.4	34.3
	50	8.0	39.0	18.8	34.2
	70	7.8	39.1	19.0	34.1

[a]Extracted from reference file of CDNN program.

4.2. Influence of ethanol on the structure of free PMA and CT–PMA

Addition of ethanol to the system results in structural changes of free PMA due to enhancement of intramolecular interaction. This is supported by a pronounced increase in the steady-state fluorescence anisotropy of pyrene-PMA (Fig. 4), a decrease in fluorescence intensity of pyrene-PMA at ethanol concentrations above 50% v/v (Figs. 2 and 3) and an increase of the relative contribution of fluorescence lifetime corresponding to inner pyrene groups of PMA at the expense of pyrene groups exposed to the solution (Table 1).

In the case of CT–PMA it is most important that the dynamic properties of the complex in water–ethanol mixtures correlate with the catalytic activity of the enzyme. It is known from the literature [8,9] that at an ethanol concentration of 20% v/v a maximal activation effect of complex formation with PE is observed. Under the same conditions, a maximal rotational correlation time of PMA segments containing CT is achieved. Thus, the activation effect can be caused by increased rigidity of the internal structure of the complex.

4.3. Influence of PMA on CT structure

In aqueous solution free A-CT is characterized by two distinct substates of the protein with different environment of the active site (τ_1 and τ_2 in Table 5). In a water–ethanol system the same two substates are present and no new substates emerge. The only parameter changed is the contribution of these substates to the equilibrium. Thus, ethanol induces a shift in equilibrium towards the substate with higher accessibility of the active site (Fig. 6). A similar conclusion can be drawn from the analysis of λ_{max} of A-CT dependence on the ethanol concentration (Fig. 5). In A-CT–PMA the active site environment of CT remains unchanged up to an ethanol concentration of 60% v/v (Fig. 5B). Moreover, using CD spectroscopy in the far-UV region, we have found that complex formation with PMA results in pronounced stabilization of the secondary structure of the enzyme in water–ethanol mixtures (Fig. 7). Stabilization was found to be more pronounced at higher CT/PMA ratios (Fig. 7C), which can be explained by the formation of a more rigid structure of the complex resulting in strong fixation of enzyme conformation.

Besides the above-mentioned structural reorganization, ethanol induces enzyme aggregation. Using TRFA, the formation of CT oligomers (trimers and tetramers) in the range of ethanol concentrations from 10 to 50% v/v was observed (Table 6A). At higher ethanol concentrations larger and insoluble protein aggregates are formed. The aggregation of CT in the range of ethanol concentrations between 40 and 80% v/v was also observed in many works [8,9,12,18,19]. Complex formation with PMA leads to suppression of enzyme aggregation up to an ethanol concentration of 60% v/v (Table 6B). A similar effect of complex formation with PE on the protein in water–cosolvent mixtures was found in [8–11].

4.4. Conclusions

In this study we have found that interaction of PMA with enzyme results in the formation of a quasi-regular compact structure of PMA on two levels: the domain structure represented by several equal segments, each containing the enzyme molecule surrounded by PE, and the globular-like overall structure (detected at high enzyme/PE ratios). Formation of such a quasi-regular structure of the complex leads to significant stabilization of the tertiary and secondary structures of the enzyme and suppression of enzyme aggregation. An increase in the rigidity of the internal structure of the complex at moderate ethanol concentrations is probably the main reason for enzyme activation under such conditions.

Acknowledgements

This research has been supported by NWO grant 047-007-005 and NATO grant LST.CLG 974984.

References

[1] A.K. Gladilin, A.V. Levashov, Biochemistry (Moscow) 63 (1998) 345–356.
[2] A.M. Klibanov, Trends Biotechnol. 16 (1997) 178–206.
[3] M.D. Snieder, Enzymes as Catalysts in Organic Synthesis, D. Reidel, Dordrecht, 1985.
[4] F.H. Arnold, Trends Biotechnol. 8 (1990) 244–249.

[5] V.V. Mozhaev, R. Lange, E.V. Kudryashova, C. Balny, Biotechnol. Bioeng. 52 (1996) 320–331.
[6] V.V. Mozhaev, E.V. Kudryashova, N. Bec, in: R. Hayashi, C. Balny (Eds.), High Pressure Bioscience and Biotechnology, Elsevier, Amsterdam, 1996, pp. 221–226.
[7] E.V. Kudryashova, V.V. Mozhaev, C. Balny, Biochim. Biophys. Acta 1386 (1998) 199–210.
[8] A.K. Gladilin, E.V. Kudryashova, A.V. Vakurov, V.A. Izumrudov, V.V. Mozhaev, A.V. Levashov, Biotechnol. Lett. 17 (1995) 1329–1334.
[9] E.V. Kudryashova, A.K. Gladilin, A.V. Vakurov, F. Heitz, A.V. Levashov, V.V. Mozhaev, Biotechnol. Bioeng. 55 (1997) 267–277.
[10] E.V. Kudryashova, I.V. Galperin, A.K. Gladilin, A.V. Levashov, in: C. Obinger, U. Burner, R. Ebermann, C. Penel, H. Greppin (Eds.), Plant Peroxidases: Biochemistry and Physiology, Rochat-Baumann, Imprimery National, Geneve, 1996, pp. 390–395.
[11] V.S. Sergeeva, E.N. Efremenko, G.M. Kazankov, A.K. Gladilin, S.D. Varfolomeev, Biotechnol. Tech. 13 (1999) 479–483.
[12] A.A. Vinogradov, E.V. Kudryashova, V.Ya. Gringerg, N.V. Grinberg, T.V. Burova, A.V. Levashov, Prot. Eng. Vol. 14 N11 (in press).
[13] V.V. Mozhaev, E.V. Kudryashova, N.V. Efremova, I.N. Topchieva, Biotechnol. Tech. 10 (1996) 621–628.
[14] Yu.L. Khmelnytsky, V.V. Mozhaev, A.B. Belova, M. Sergeeva, K. Martinek, Eur. J. Biochem. 198 (1991) 31–41.
[15] V.V. Mozhaev, M. Sergeeva, A.B. Belova, Yu.L. Khmelnytsky, Biotechnol. Bioeng. 35 (1990) 653–659.
[16] V.V. Mozhaev, Yu.L. Khmelnitsky, M.A. Sergeeva, A.B. Belova, N.L. Klyachko, A.V. Levashov, K. Martinek, Eur. J. Biochem. 184 (1989) 597–602.
[17] M. Sato, T. Sasaki, M. Kobayashi, H. Kise, Biosci. Biotechnol. Biochem. 64 (2000) 2552–2558.
[18] T. Kijima, S. Yamamoto, H. Kise, Enzyme Microb. Technol. 18 (1996) 2–6.
[19] Y. Tomiuchi, T. Kijima, H. Kise, Bull. Chem. Jpn. 66 (1993) 1176–1181.
[20] A. Katchalsky, H.J. Eisenberg, Polym. Sci. 6 (1951) 145–150.
[21] L. Leclercq, A. Pollet, M. Morcellet, B. Martel, Eur. Polym. J. 36 (1999) 185–193.
[22] Yo. Muroga, T. Yashida, S. Kawaguchi, Biophys. Chem. 81 (1999) 45–57.
[23] C. Heitz, M. Rawiso, J. Francoi, Polymer 40 (1999) 1637–1650.
[24] J. Broos, A.J. Visser, J. Engbersen, W. Verboom, A. Van Hoek, D. Reinhoudt, J. Am. Chem. Soc. 117 (1995) 12657–12663.
[25] V.N. Dorovska-Taran, C. Veeger, A.J.W.G. Visser, Eur. J. Biochem. 211 (1993) 47–55.
[26] V.A. Izumrudov, S.I. Kargov, M.V. Zhiryakova, A.B. Zezin, V.A. Kabanov, Biopolymers 35 (1994) 523–531.
[27] R.P. Haugland, L. Stryer, in: G.N. Ramachandran (Ed.), Conformation of Biopolymers, Academic Press, New York, 1967, p. 321.
[28] G.R. Schonbaum, B. Zerner, M. Bender, J. Biol. Chem. 236 (1961) 2930–2938.
[29] H.E.W. Pap, P.I.H. Bastiaens, J.-W. Borst, P.A.W. van der Berg, A. van Hoek, G.T. Snoek, K.W.A. Wirtz, A.J.W.G. Visser, Biochemistry 32 (1993) 13310–13317.
[30] A. van Hoek, K. Vos, A.J.W.G. Visser, IEEE J. Quant. El. QE-23 (1987) 1812–1819.
[31] K. Vos, A. van Hoek, A.J.W.G. Visser, Eur. J. Biochem. 165 (1987) 55–63.
[32] Y.-M. Liou, F. Fuchs, Biophys. J. 61 (1992) 892–901.
[33] V. Glushko, M.S.R. Thaler, C.D. Karp, Arch. Biochem. Biophys. 210 (1981) 33–42.
[34] E.H.W. Pap, A. Hanicak, A. van Hoek, K.W.A. Wirtz, A.J.W.G. Visser, Biochemistry 34 (1995) 9118–9125.
[35] J.R. Lakowicz, Principles of Fluorescence Spectroscopy, 2nd edn., Plenum Press, New York, 1999.
[36] V.A. Izumrudov, Yu. Galaev, B. Mattiasson, Bioseparation 7 (1999) 207–220.
[37] Yu.L. Khmelnitsky, A. van Hoek, C. Veeger, A.J.W.G. Visser, J. Phys. Chem. 93 (1989) 872–878.
[38] A. Shibata, M. Yamamoto, T. Yamashita, J.-S. Chiou, H. Kamaya, I. Ueda, Biochemistry 31 (1992) 5728–5733.
[39] M. Buch, S.E. Radford, C.M. Dobson, Biochemistry 32 (1993) 669–678.